

LETTER TO THE EDITOR

Lyman Continuum escaping from in-situ formed stars in a tidal bridge at $z = 3$

T. E. Rivera-Thorsen^{1,*}, A. Le Reste², M. J. Hayes³, S. Flury³, A. Saldana-Lopez¹, B. Welch⁴, S. Choe¹, K. Sharon⁵, K. Kim⁶, M. R. Owens⁷, E. Solhaug^{8,9}, and H. Dahle¹⁰

¹ The Oskar Klein Centre, Department of Astronomy, Stockholm University, AlbaNova, 10691 Stockholm, Sweden

² Minnesota Institute for Astrophysics, University of Minnesota, 116 Church Street SE, Minneapolis, MN 55455, USA

³ Institute for Astronomy, University of Edinburgh, Royal Observatory, Edinburgh, EH9 3HJ, UK

⁴ International Space Science Institute, Hallerstrasse 6, 3012 Bern, Switzerland

⁵ Department of Astronomy, University of Michigan, 1085 S. University Ave, Ann Arbor, MI 48109, USA

⁶ IPAC, California Institute of Technology, 1200 E. California Blvd., Pasadena CA, 91125, USA

⁷ Department of Astronomy, University of California, Berkeley, Berkeley, CA 94720, USA

⁸ Department of Astronomy and Astrophysics, University of Chicago, 5640 South Ellis Avenue, Chicago, IL 60637, USA

⁹ Kavli Institute for Cosmological Physics, University of Chicago, Chicago, IL 60637, USA

¹⁰ Institute of Theoretical Astrophysics, University of Oslo, P.O. Box 1029, Blindern, NO-0315 Oslo, Norway

ABSTRACT

In order to account for reionization of the early Universe, galaxies at that time must have had significantly higher escape fractions of Lyman Continuum (LyC) than observed in the present Universe. Any explanation invoked to explain LyC escape must agree with this dramatic cosmic evolution. Galaxy mergers are often suggested as such a regulating mechanism. They occur an order or magnitude more frequently at $z \gtrsim 3$ than in the local Universe, and they can trigger LyC escape either by inducing strong nuclear starbursts, or by tidally displacing the neutral ISM from the bulk of the stars. In the local Universe, LyC escape has been found to correlate with a range of physical and observable properties closely associated with strong star formation. For this reason, interest in mergers as drivers of LyC escape have been mainly focused on their capacity to induce strong star formation. However, at $z \gtrsim 2$, these correlations are weaker, and we observe a much more diverse Lyman Continuum Emitter (LCE) population. This suggests that processes external to the LCE galaxies are more important for facilitating the escape at higher redshifts, which makes tidal displacement an interesting explanatory model; however, this has only been conclusively observed once before. In this letter, we present archival JWST/NIRSpec IFU and HST UVIS and IR imaging observations of the $z = 3$ Lyman-Continuum emitter LACES104037. We find that its Lyman-Continuum escape originates in a tidal bridge in the direction towards an interacting companion galaxy first identified in this work. LyC escape from tidal stripping or in-situ formed stars in tidal features could help explain both the higher cosmic LyC escape fraction and the greater diversity of LCE galaxy properties at higher redshifts.

Key words. Galaxies: kinematics and dynamics—Galaxies: starburst—Galaxies: star formation—Galaxies: interactions—Galaxies: individual: LACES104037

1. Introduction

Young, star-forming galaxies contributed a major part of the ionizing Lyman-Continuum (LyC) photons that re-ionized the intergalactic medium (IGM) in what is now known as the Epoch of Reionization (EoR), the last major phase transition of the Universe (e.g., Faucher-Giguère 2020; Haardt & Madau 2012; Wise 2019). Estimates of the cosmic LyC escape fraction ($f_{\text{esc}}^{\text{LyC}}$) required to account for the EoR are centered around 10–20% (Robertson et al. 2015; Naidu et al. 2020; Giovinazzo et al. 2025); some estimates go higher (Davies et al. 2021), while some go as low as $f_{\text{esc}}^{\text{LyC}} \sim 5\%$ (Finkelstein et al. 2019; Atek et al. 2024). At low redshifts, the average escape fraction is consistently far below these values. At $z \lesssim 0.1$ it is negligible, with only two known Lyman-Continuum emitter (LCE) galaxies, each with $f_{\text{esc}} \lesssim 5\%$ (Puschignig et al. 2017; Komarova et al. 2024). In the low-redshift Universe, $z \lesssim 0.4$, about 70 LCEs are known, some of which have very high escape fractions (e.g., Borthakur et al. 2014; Izotov et al. 2018, 2025; Flury et al. 2022a; Malkan & Malkan 2021); but

they are rare and the cosmic escape fraction is very low. Stacking analyses at $z \sim 1$ and $z \sim 3$ have consistently shown upper limits to the average escape fraction well below what is required to account for the EoR (Cowie et al. 2009; Rutkowski et al. 2016; Grazian et al. 2017; Alavi et al. 2020).

Strong LyC escape depends on a high production rate of ionizing photons, and on mechanisms carving out channels through the neutral ISM to enable the free passage of LyC photons into the IGM (e.g., Trebitsch et al. 2017; Kakiichi & Gronke 2021). In the low-redshift Universe, LyC escape has been found to correlate with observables such as the UV β slope, reflecting low dust content and a young stellar population with high LyC production rate (Ji et al. 2020; Kim et al. 2020; Flury et al. 2022b, 2025); with $[\text{O III}]/[\text{O II}]$ ratio, which reflects the ionization level of the ISM (Izotov et al. 2018; Flury et al. 2022a); with weak neutral absorption features, reflecting low H I column density along the line of sight (Chisholm et al. 2018; Gazagnes et al. 2020; Saldana-Lopez et al. 2022); and with broad emission line components reflecting strong bulk outflows which can rupture the H I envelope around the source star cluster (Alexandroff et al. 2015; Chisholm et al.

* Corresponding author. e-mail: trive@astro.su.se

2017; Mainali et al. 2022; Amorín et al. 2024). However, many of these correlations predicting $f_{\text{esc}}^{\text{LyC}}$, such as $[\text{O III}]/[\text{O II}]$, β_{UV} , and Ly α equivalent width, are weakened or break down at $z \gtrsim 2$ (Zhu et al. 2025; Giovinazzo et al. 2025; Rivera-Thorsen et al. 2022; Saxena et al. 2022; Bassett et al. 2022; Kerutt et al. 2024; Mascia et al. 2025; Citro et al. 2025), leaving a more diverse population of leakers observed at higher redshifts. This shift to a more diverse leaker population suggests that LyC escape at these redshifts depends less on intrinsic properties of the leaking galaxies themselves, and more on factors external to the leaking galaxies, than at lower redshifts.

Mergers and major interactions have been suggested by multiple authors as triggers of LyC escape, as they can both induce strong star formation and displace stars from gas (e.g., Bridge et al. 2010; Bergvall et al. 2013; Le Reste et al. 2024); and indeed, the cosmic rate of mergers and major interactions has been found to rise by an order of magnitude from $z \sim 0.3$ to $z \sim 3$, after which it stays within a factor of a few, roughly consistent with the evolution in $f_{\text{esc}}^{\text{LyC}}$ (Puskás et al. 2025; Duan et al. 2025). Indeed, in the $z \sim 0.3$ Low-Redshift Lyman Continuum Sample, follow-up imaging has shown that at least 40% of these galaxies show signs of undergoing mergers (Le Reste et al. 2025), a strong overrepresentation compared to the $\sim 5\%$ of the general low-redshift population (e.g. Darg et al. 2010). (Kostyuk & Ciardi 2024) found that simulated galaxies at $6 \lesssim z \lesssim 10$ had an average $f_{\text{esc}} \sim 15\%$ if they were merging, compared to $\sim 3\%$ if they were not. Observationally, Zhu et al. (2025) found from visual classification that 20 of 23 LCEs at $z \sim 3$ in GOODS-South were undergoing mergers. In contrast, (Mascia et al. 2025) compared the merger rate of a number of EoR galaxies to statistical tracers of LyC escape and found that there was no statistical correlation between them; however, these authors relied on observable LCE tracers calibrated in the local Universe. While they did adjust for known cosmic evolution of these tracers, such an analysis is still left vulnerable to any unknown biases built-in to these local calibrations, biases which are evident from the increased diversity of LCEs observed at $z \gtrsim 3$. In both works, it should also be noted that $z \gtrsim 2$ merger classification from imaging data alone is notoriously difficult and prone to false positives, due to more compact and clumpy galaxies. Mergers can lead to LyC escape through either induced bursty star formation or spatial displacement of neutral gas from the bulk of the galaxy’s stars. Merger induced central starbursts are not qualitatively different from other starbursts, and thus should not give rise to any deviation from the correlations between LCE and bursty star formation established at low redshifts. In contrast, tidal displacement of neutral ISM from the bulk of the stars and possible in-situ star formation in outer regions of a galaxy, leads to less dependence on intrinsic galaxy properties of LyC escape, and can potentially give rise to the observed diversity of LCE galaxies observed at $z \gtrsim 2$. However, such scenarios have barely been studied observationally. One example of LyC escape facilitated by tidal stripping of H I during a major merger was first observed directly in the nearby galaxy Haro 11 by (Le Reste et al. 2024; Ejdetjärn et al. 2025); and Rivera-Thorsen et al. (2025) reported circumstantial evidence for a similar scenario in the gravitationally lensed $z = 2.37$ Sunburst Arc. In this work, we present observational evidence for Lyman Continuum escaping from young stars formed in situ in a tidal bridge extending from a starburst galaxy at $z = 3$, towards a spectroscopically confirmed interacting companion, suggesting that such configurations might be more common than previously thought.

We assume a standard flat Λ CDM cosmology with $H = 70 \text{ km s}^{-1} \text{ Mpc}^{-1}$ and $\Omega_{\text{M}} = 0.3$. Images are oriented North up, East left.

2. Target and observations

LACES104037 was first reported as an LCE by Fletcher et al. (2019). These authors classified it as part of their “silver” sample because the offset between the observed emission in F336W and the core of the galaxy as seen in F160W was slightly more than $0.6''$, which they associate with an elevated risk that the observed UV emission originates from an interloper. It was selected as a target for NIRSpec IFU observations in Cycle 1 (PID 01827; PI: Kakiichi) for its F160W morphology, which is among the more extended and complex in the sample of Fletcher et al..

LACES104037 was observed on October 27th 2022, using JWST NIRSpec in IFU mode using the F170LP/G235M filter/grating combination. We downloaded the Level 3 spectral cubes from MAST. We have not attempted any further reduction or cleaning steps than what have been done by the automated pipeline, except for manually aligning and subtracting the background cube.

We also obtained archival HST imaging data from the LymAn Continuum Escape Survey (LACES, PID: 14747, PI: Robertson), taken with WFC3/F336W and ACS/F160W. These data are described by Fletcher et al. (2019); we refer to that paper for a description of the observations. Specifically, for UVIS/F336W, we obtained the Hubble Advanced Products - Multi Visit Mosaic (HAP-MVM) products from MAST, which offered a convenient high-quality data product. We obtained the combined ACS/F160W frames from the Hubble Legacy Archive (HLA). The WCS systems were well aligned in F336W and NIRSpec already, but was somewhat off in F160W. We used a number of compact sources in the field to make sure F160W was aligned to the other observations to within $\sim 0''.05$.

3. Analysis and results

3.1. Stellar morphology

LACES 104037 and surroundings as seen in these observations are shown together in figure 1. The left panel shows restframe B band F160W imaging, the center panel shows restframe LyC F336W imaging, and the right panel shows the wavelength-median image of the NIRSpec cube. The NIRSpec footprint is shown in green in the HST image panels; the inset axes show zoom-ins centered on the site of LyC escape. F160W shows a galaxy with two bright cores separated by $0''.3$ along the SE-NW direction, and an apparent tidal tail protruding from its SE edge, pointing toward another galaxy to the S at the edge of the NIRSpec footprint. The center panel shows that the LyC emission is spatially coincident with the apparent tidal tail, rather than the main star forming clumps in the central regions of the galaxy. The LyC centroid is offset from the mid point between the two central knots by $\approx 0''.62$.

3.2. Emission line mapping

We performed line fits of the emission lines of LACES104037 in each spaxel of the NIRESpec IFU cube following the procedure described in Rivera-Thorsen et al. (2025), which we refer to for a more detailed description. In short, we initially subtracted the continuum in each spaxel by masking out the strong emission lines, subsequently taking a running median in a 31 pixel

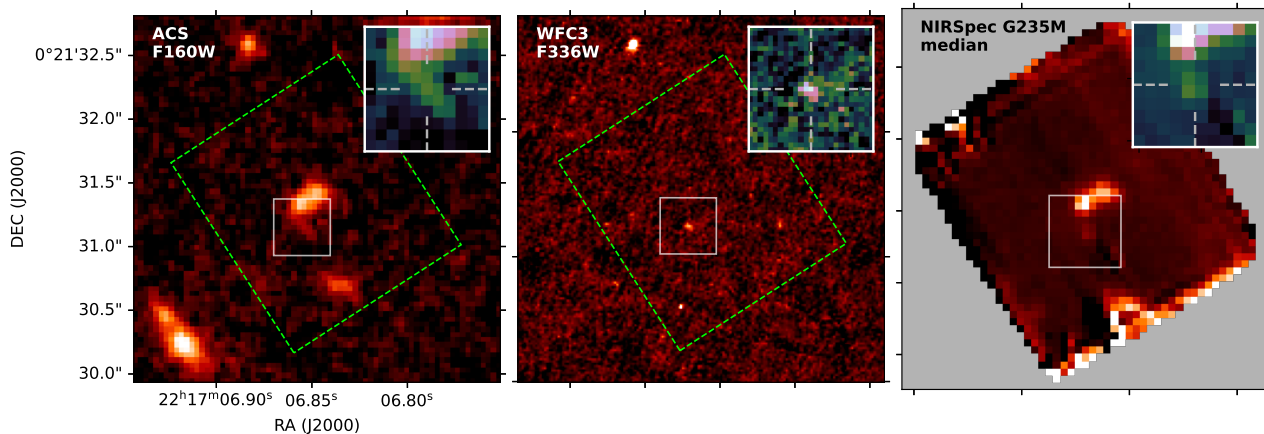


Fig. 1: Archival Hubble observations in F160W probing the rest-frame B band (left) and F336W showing rest-frame LyC (center), along with a wave-axis median image of the JWST/NIRSpec IFU cube showing the rest-frame Optical (right), showing LACES104037 and its immediate surroundings. Green dashed squares in the HST images show the approximate footprint of the JWST/NIRSpec observations. Insets show a zoom in on the LACES104037 itself, centered on the LCE.

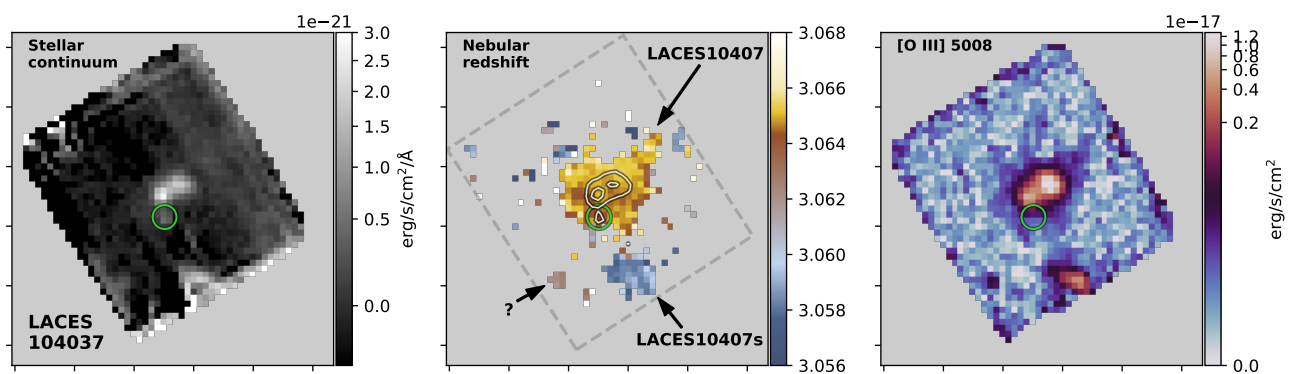


Fig. 2: Kinematics and [O III] line emission in LACES104037 and the companion LACES104037s. The Redshift is masked to only include spaxels where $S/N([O\ III]) > 3$ and the line fitting successfully converged on a solution. This map shows that LACES104037s is close to LACES104037 in velocity space and most likely an interacting companion. The green circle shows the approximate location of the escaping LyC, and the white contours in the redshift map show stellar continuum levels from the left panel.

window, interpolating this onto the masked pixel, and subtracting this running median. We then used the line fitting software `CubeFitter.jl` (Rivera-Thorsen 2025) to simultaneously fit the lines $H\beta$, $[O\ III]\lambda\lambda\ 4960, 5008$, $H\alpha$, and $[N\ II]\lambda\lambda\ 6548, 6584$ to a shared redshift and line width. We subsequently fitted a number of fainter lines including $[S\ II]\lambda\lambda\ 6718, 6731$, assuming the same kinematic properties. The G235M grating does not resolve the relevant line widths of this galaxy; hence, even though the fits did yield nominal line widths, they are not reliable. In addition to the line fits, we have also computed line fluxes by numerical integration. In Figure 2, we show resulting kinematic and line emission maps. The left panel shows the stellar continuum represented by the median along the wavelength axis in each spaxel. The green circle marks the location of the escaping LyC, while the contours show continuum emission from the left panel. The center panel shows the best-fit redshift in each spaxel. Importantly, the fitting shows that the visual companion galaxy to the S of LACES104037 is indeed a physical, interacting companion, separated from LACES104037 by a projected distance of ~ 12.5 kpc (approximately $1.5 \times$ the radius of the Milky Way disk); and blueshifted by a relative line-of-sight velocity of

$\sim 450\text{ km s}^{-1}$. We found no designation for this companion in NED, so we designate it LACES104037s for now. We also note a small group of spaxels to the SE with redshift in between the two major galaxies; possibly a third, minor interacting party. The right panel shows the $[O\ III]\lambda\ 5008$ numerical line flux map. This map shows a faint, continuous bridge of ionized gas between LACES104037 and the companion galaxy, and significant emission in both. We note that the LyC escape is not coincident with locally elevated emission strength in [O III]. Stars and gas are often separated in tidal features (Hibbard et al. 2000); so plausibly, the amount of gas in the tidal bridge is small and relatively easy for stellar wind from young stars to have cleared away. If this is a common occurrence in the $z \gtrsim 2$ Universe, it could constitute a significant source of ionizing radiation not well accounted for by low-redshift calibrations.

3.3. Ionizing escape fraction and stellar population age

We estimated a the global escape fraction from the LCE clump by comparing the $H\alpha$ and LyC flux. We extracted a spectrum from the 2×2 IFU spaxels seen in the crosshairs in the right

panel of Figure 1, approximately centered on the LCE, measured the $H\alpha$ line flux, and used the conversion factor from Kennicutt (1998) to translate this into a ionizing photon flux $q(H^0)$. We measured the LyC flux in a matching aperture, and estimated the photometric errors as the standard deviation of 500 randomly placed apertures on empty nearby regions. We converted LyC flux to an ionizing photon flux using the photon energy at 825 Å, the redshift-corrected central wavelength in F336W. We found a $F(H\alpha) = (4.7 \pm 0.2) \times 10^{-19}$ erg cm $^{-2}$ s $^{-1}$ yielding $q(H\alpha) = (2.7 \pm 0.1) \times 10^{-7}$ cm $^{-2}$ s $^{-1}$; and $F(\text{LyC}) = (8.7 \pm 1.9) \times 10^{-18}$ erg cm $^{-2}$ s $^{-1}$ yielding $q(\text{LyC}) = (3.62 \pm 0.79) \times 10^{-7}$ cm $^{-2}$ s $^{-1}$. Assuming no significant dust extinction and no LyC flux outside the wavelength range of the filter, this leads to $f_{\text{esc}}^{\text{LyC}} = 0.57 \pm 0.05$. We also estimated $W(H\alpha)$ in this spectrum, taking into account the ionizing escape fraction. We found an approximate redshift- and LyC escape-corrected $W(H\alpha) \approx 339 \pm 48$ Å. Comparing this to an instantaneous burst S99 model with a fiducial metallicity of 20% Z_{\odot} , we find an approximate stellar age of $\sim 6 - 7$ Myr.

3.4. Galaxy interaction timescale

The two interacting galaxies have redshifts of $z_{\text{Comp}} \approx 3.059$ and $z_{\text{LACES104037}} \approx 3.065$, yielding a relative LOS velocity component between the two galaxies of $v_{\parallel} = v_{\text{rel}} \times \cos \theta \approx 445$ km s $^{-1}$, where θ is the viewing angle. The transverse physical distance component between the galaxies is $d_{\perp} = d \times \sin \theta \approx 12.5$ kpc. From this, the time since interaction is given as $t = dv_{\text{rel}}^{-1} = d_{\perp} v_{\parallel}^{-1} (\tan \theta)^{-1} \approx 27$ Myr $(\tan \theta)^{-1}$. We do not know the viewing angle of the relative motion, but reasonable angles of 30 and 60 deg correspond to a time since closest approach of $t \approx 45$ and $t \approx 15$ Myr. We also consider the possibility that the dual cores might mean LACES104037 is already a late-stage merger, and the tidal tail might instead originate from this interaction. However, while the separation from LyC to the nearest clump is only 0'36, the velocity is $v \lesssim 80$ km s $^{-1}$, leading to a travel time of $t \approx 34$ Myr $\times (\tan \theta)^{-1}$ Myr. Since the stellar population age is $\lesssim 6.5$ Myr, it is unlikely that the leaking stars existed already at the time of closest approach; instead, they have likely formed inside the tidal bridge formed by the interaction.

4. Summary

We have compared archival HST imaging and JWST NIRSpec IFU observations of the galaxy LACES104037. We report that a galaxy at a projected angular distance of $\approx 1''.7$, which is partially inside the IFU footprint, is in fact an interacting companion which we designate LACES1034037s, at a transverse physical distance of ≈ 12.5 kpc, and a line-of-sight relative velocity of ≈ 450 km s $^{-1}$. We find that LACES104037 differs from typical LCEs at low redshift in that the escaping LyC originates, not from the bright and highly star forming core, but from an in-situ formed star cluster in a tidal bridge toward the companion, offset from the center of the galaxy by *approx* 4.8 kpc projected distance, in a region not associated with elevated nebular line emission. We find traces of a possible third, smaller companion system to the SE of the main companion galaxy, with a redshift in between the two larger galaxies. We find faint but definite, extended line emission tendrils and halos surrounding both the major galaxies, marginally overlapping between them.

This suggests that a—potentially significant—subpopulation of LCE galaxies, particularly at $z \gtrsim 2$, might not be well characterized by the $z \lesssim 0.5$ samples typically used to calibrate observational $f_{\text{esc}}^{\text{LyC}}$ proxies.

Our result also calls attention to the possibility that surveys might be selecting against a system like LACES104037, and potentially many more. Merging systems are often excluded due to the risk that the companion might be an interloper; in particular when LyC is found spatially offset from the main stellar body of the galaxy. While such a cautious approach certainly has merit, this work shows that it might also lead to exclusion of a significant number of LCEs and consequently an underestimation of the cosmic escape fraction.

Acknowledgements. This work is based on observations made with the NASA/ESA/CSA James Webb Space Telescope and Hubble Space Telescope. The data were obtained from the Mikulski Archive for Space Telescopes at the Space Telescope Science Institute, which is operated by the Association of Universities for Research in Astronomy, Inc., under NASA contract NAS 5-03127 for JWST. These observations are associated with programs 14747 and 01827. ER-T is supported by the Swedish Research Council grant 2022-04805.

References

- Alavi, A., Colbert, J., Teplitz, H. I., et al. 2020, *ApJ*, 904, 59
 Alexandroff, R. M., Heckman, T. M., Borthakur, S., Overzier, R., & Leitherer, C. 2015, *ApJ*, 810, 104
 Amorín, R. O., Rodríguez-Henríquez, M., Fernández, V., et al. 2024, *A&A*, 682, L25
 Atek, H., Labbé, I., Furtak, L. J., et al. 2024, *Nature*, 626, 975
 Bassett, R., Ryan-Weber, E. V., Cooke, J., et al. 2022, *MNRAS*, 511, 5730
 Bergvall, N., Leitert, E., Zackrisson, E., & Marquart, T. 2013, *A&A*, 554, A38
 Borthakur, S., Heckman, T. M., Leitherer, C., & Overzier, R. A. 2014, *Science*, 346, 216
 Bridge, C. R., Teplitz, H. I., Siana, B., et al. 2010, *ApJ*, 720, 465
 Chisholm, J., Gazagnes, S., Schaerer, D., et al. 2018, *A&A*, 616, A30
 Chisholm, J., Orlitová, I., Schaerer, D., et al. 2017, *A&A*, 605, A67
 Citro, A., Scarlata, C. M., Mantha, K. B., et al. 2025, *ApJ*, 986, 184
 Cowie, L. L., Barger, A. J., & Trouille, L. 2009, *ApJ*, 692, 1476
 Darg, D. W., Kaviraj, S., Lintott, C. J., et al. 2010, *MNRAS*, 401, 1043
 Davies, F. B., Bosman, S. E. I., Furlanetto, S. R., Becker, G. D., & D'Aloisio, A. 2021, *ApJ*, 918, L35
 Duan, Q., Conselice, C. J., Li, Q., et al. 2025, *MNRAS*, 540, 774
 Ejdejtjärn, T., Agertz, O., Renaud, F., et al. 2025, *MNRAS*, 543, 3849
 Faucher-Giguère, C.-A. 2020, *MNRAS*, 493, 1614
 Finkelstein, S. L., D'Aloisio, A., Paardekooper, J.-P., et al. 2019, *ApJ*, 879, 36
 Fletcher, T. J., Tang, M., Robertson, B. E., et al. 2019, *ApJ*, 878, 87
 Flury, S. R., Jaskot, A. E., Ferguson, H. C., et al. 2022a, *ApJS*, 260, 1
 Flury, S. R., Jaskot, A. E., Ferguson, H. C., et al. 2022b, *ApJ*, 930, 126
 Flury, S. R., Jaskot, A. E., Saldana-Lopez, A., et al. 2025, *ApJ*, 985, 128
 Gazagnes, S., Chisholm, J., Schaerer, D., Verhamme, A., & Izotov, Y. 2020, *A&A*, 639, A85
 Giovinazzo, E., Oesch, P. A., Weibel, A., et al. 2025, *arXiv e-prints*, arXiv:2507.01096
 Grazian, A., Giallongo, E., Paris, D., et al. 2017, *A&A*, 602, A18
 Haardt, F. & Madau, P. 2012, *ApJ*, 746, 125
 Hibbard, J. E., Vacca, W. D., & Yun, M. S. 2000, *AJ*, 119, 1130
 Izotov, Y. I., Schaerer, D., Worseck, G., et al. 2025, *arXiv e-prints*, arXiv:2510.22152
 Izotov, Y. I., Worseck, G., Schaerer, D., et al. 2018, *MNRAS*, 478, 4851
 Ji, Z., Giavalisco, M., Vanzella, E., et al. 2020, *ApJ*, 888, 109
 Kakiichi, K. & Gronke, M. 2021, *ApJ*, 908, 30
 Kennicutt, R. C. 1998, *Annual Review of Astronomy and Astrophysics*, 36, 189–231
 Kerutt, J., Oesch, P. A., Wisotzki, L., et al. 2024, *A&A*, 684, A42
 Kim, K., Malhotra, S., Rhoads, J. E., Butler, N. R., & Yang, H. 2020, *ApJ*, 893, 134
 Komarova, L., Oey, M. S., Hernandez, S., et al. 2024, *ApJ*, 967, 117
 Kostyuk, I. & Ciardi, B. 2024, *arXiv e-prints*, arXiv:2412.04348
 Le Reste, A., Cannon, J. M., Hayes, M. J., et al. 2024, *MNRAS*, 528, 757
 Le Reste, A., Jaskot, A. E., Brazie, J., et al. 2025, *arXiv e-prints*, arXiv:2509.06922
 Mainali, R., Rigby, J. R., Chisholm, J., et al. 2022, *ApJ*, 940, 160
 Malkan, M. A. & Malkan, B. K. 2021, *ApJ*, 909, 92
 Mascia, S., Pentericci, L., Llerena, M., et al. 2025, *A&A*, 701, A122
 Naidu, R. P., Tacchella, S., Mason, C. A., et al. 2020, *ApJ*, 892, 109
 Puschnig, J., Hayes, M., Östlin, G., et al. 2017, *MNRAS*, 469, 3252
 Puskás, D., Tacchella, S., Simmonds, C., et al. 2025, *MNRAS*, 540, 2146
 Rivera-Thorsen, T. E. 2025, *thriveth/CubeFitter.jl: Initialize DOI and add logo*
 Rivera-Thorsen, T. E., Hayes, M., & Melinder, J. 2022, *A&A*, 666, A145
 Rivera-Thorsen, T. E., Welch, B., Hutchison, T., et al. 2025, *arXiv e-prints*, arXiv:2510.11702
 Robertson, B. E., Ellis, R. S., Furlanetto, S. R., & Dunlop, J. S. 2015, *ApJ*, 802, L19
 Rutkowski, M. J., Scarlata, C., Haardt, F., et al. 2016, *ApJ*, 819, 81
 Saldana-Lopez, A., Schaerer, D., Chisholm, J., et al. 2022, *A&A*, 663, A59
 Saxena, A., Pentericci, L., Ellis, R. S., et al. 2022, *MNRAS*, 511, 120
 Trebitsch, M., Blaizot, J., Rosdahl, J., Devriendt, J., & Slyz, A. 2017, *MNRAS*, 470, 224
 Wise, J. H. 2019, *Contemporary Physics*, 60, 145
 Zhu, S., Zheng, Z.-Y., Yuan, F.-T., Jiang, C., & Lin, R. 2025, *ApJ*, 982, L58